Bull. Mater. Sci., Vol. 34, No. 1, February 2011, pp. 97–104. © Indian Academy of Sciences.

Polycarboxylate derivative of α-amino acid as growth modifier of sulphide minerals

HARJYOTI THAKURIA and GOPAL DAS*
Department of Chemistry, Indian Institute of Technology Guwahati, Guwahati 781 039, India

MS received 10 July 2007; revised 2 January 2011

Abstract. Construction of modified inorganic mineral with controlled mineralization analogues of those produced by nature is now of current interest for understanding the mechanism of the *in vivo* biomineralization processes, as well as looking for fresh industrial and technological applications. Low-molecular-weight chiral polycarboxylate ligands derived from naturally occurring *L*-α-amino acids have been used as model systems to study the effect of small organic matrix on crystal growth modification. The sulphide minerals are characterized by PXRD, FT–IR and SEM. Furthermore, the optical properties of these minerals have been characterized by UV-Vis and photoluminescence (PL) spectra.

Keywords. Biomineralization; organic matrix; low-molecular-weight chiral polycarboxylate; sulphide mineral; photoluminescence.

1. Introduction

Fabrication of nano- to microscopic-scale inorganic materials with special size and morphology are of great interest for materials chemistry due to their importance in basic scientific research and potential technological applications (Alivisatos 1996; Hu *et al* 1999; Puntes *et al* 2001; Chen and Carroll 2002; Sun and Xia 2002; Wang *et al* 2003). In the past few decades, there have been an increasing number of reports on the synthesis of inorganic crystals of various size and shape (Xia and Yang 2003; Xiong *et al* 2004; Yu *et al* 2004; Zhang *et al* 2004). Studies on the shape control of inorganic crystals will, to some extent, give insights into the crystallization behaviour in a nano- or micro-sized scale owing to the traditional lack of understanding of the growth history and shape evolution process. Template-directed synthesis of inorganic minerals are the most common and important phenomena in living organisms.

Sulfides of metals have been extensively studied for their outstanding properties and potential use in future devices (Xie *et al* 1999; Barnett and Landman 1997; Kuang *et al* 2003). Cadmium sulphide (CdS) is a technologically useful material, as many devices based on CdS, including sensors have come up in recent years. Cadmium sulfide, a direct bandgap semiconductor with E_g of 2·42 eV (Suresh *et al* 2005; Khanna *et al* 2005; Pentimalli *et al* 2005) at room temperature, can be used for photoelectronic devices. CdS powder is used in the production of light sources emitting from the green region, in the technology of solar cells and photocells (Grus and Sikorska 1999), X-ray detector, as a photo catalyst, chemical or biological sensor, ceramics, magnetic storage, LED, displays, molecular level lubrications and others (Wintera *et al* 2004; Raji *et al* 2005). Lead sulphide (PbS) is another interesting material with an exciton Bohr radius of 9 nm and a bulk bandgap of 0·41 eV, corresponding to an optical cut-off of 3020 nm (Liu *et al* 2003a, b). PbS has been used in IR detectors and have different utility in different fields, e.g. it is used in photoresistor, photovoltaic devices, heterojunction diode, electroluminescent layers and surface acoustic wave devices. Chalconides of lead sulphide have proved their potential as efficient absorbers of electromagnetic radiation. Lead sulphide is also used as IR-detector (Suresh *et al* 2005). Zinc sulphide is used in the microelectronic devices, chemical or biological sensors, light-emitting devices and displays, molecular level lubrications (Yang and Lieber 1996; Labrenz *et al* 2000; Ma *et al* 2004).

Morphosynthesis strategies inspired by biomineralization processes give access to a wide range of fascinating and useful crystalline meso- and/or nanostructures (Mann *et al* 1993; Mo *et al* 2002; Panda *et al* 2007). In recent years, mechanism of biomineralization has been intensely studied with the aim of understanding how crystal polymorph and structural features can be controlled by organic additives. This research is inspired by the fascinating mechanical and optical properties of biominerals and their complex forms, and the exquisite control of crystallization over several length scales in biomineralization processes.

We were interested in exploring the utility of low-molecular-weight organic molecules as crystal growth modifier as well as to understand their role to regulate the

*Author for correspondence (gdas@iitg.ernet.in)

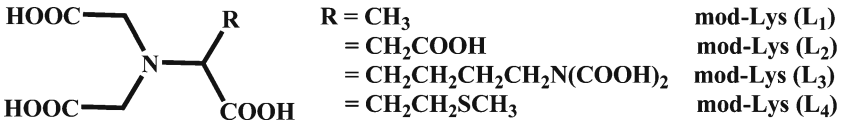

Scheme 1.

kinetics of crystal nucleation and growth. In our lab, we are also preparing different inorganic minerals using various other types of templates, viz. biological gel, peptide extracted from biological sources and microorganism. Carboxylic acids are known to display Cd^{2+}, Zn^{2+} and Pb^{2+} binding that can potentially either nucleate the growth of a given mineral or interact strongly and specifically with growing crystal faces, thus altering the morphology of the crystals in a controlled fashion. We report here the use of some low-molecular-weight chiral polycarboxylate ligands (Borah *et al* 2006) derived from naturally occurring *L*-α-amino acids as templates for crystal growth modifiers in the processes of mineralization.

2. Experimental

2.1 *Materials*

The cadmium acetate, zinc acetate and lead acetate were analytically pure. The water used in the experiment was the milli-Q water. Analytically pure ferrous sulphide and dilute sulphuric acid was used for the production of hydrogen sulphide gas. Synthesis and characterization of the ligands L_{1-3} (Borah *et al* 2006) were reported earlier and that of L_4 is reported here (see scheme 1).

2.2 *Synthesis of ligands L_4 [2-(bis-carboxymethyl-amino)-4-methylsulfanyl-butyric acid]*

N-alkylation of *L*-methionine was done by treating them with chloro acetic acid at basic pH. An aqueous solution of chloro acetic acid was added to the solution of *L*-α-amino acid in Milli-Q water ($\sim$1 mM) in a round-bottomed flask and stirred for $\sim$15 min at *RT* to make the solution homogeneous. The resulting solution was refluxed. The pH of the solutions was maintained at $\sim$10 for 2 h. The resulting solution was then concentrated to about half of the original volume under reduced pressure. On cooling, a precipitate of NaCl started forming. The precipitate was filtered and filtrate was acidified with dilute hydrochloric acid and kept overnight for recrystallization. Crystals were collected by filtration and dried *in vacuo*. Yield: 45%, m.p.: 320°C; ESI–MS, *m*/*z*(%): 265 (80) $[L_4]^+$; Analysis–Calcd. for $C_9H_{15}NO_6S$: C, 40·75; H, 5·70; N, 5·28; S, 12·09. Found: C, 41·21; H, 5·21; N, 4·91; S, 12·57. ^{1}H NMR (400 MHz, D_2O, 25°C, TMS) δ (ppm): 1·9 (*m*, 2H), 2·1 (*s*, 3H), 2·5 (*t*, 2H), 3·3 (*s*, 4H), 5·6 (*t*, 1H), ^{13}C NMR (100 MHz, D_2O, 25°C, TMS) δ (ppm): 17·2, 29·5, 30·2, 56·2, 63·4, 174·2, 177·1.

2.3 *Crystallization experiments*

For each set of the mineral and ligand composition we have performed three parallel reactions: simple Milli-Q water system (control), *L*-α-amino acid system (control) and polycarboxylate ligand system. In a typical experiment, 0·001 M ligand solution is mixed with 0·01 M metal acetate salt solution in Milli-Q water. The mixture is made alkaline by ammonia solution and pH is maintained within 7·2–8·6 range and kept at *RT* for 12 h without stirring at 25$\pm$2°C. Then the mixture was placed in a closed container filled with H_2S gas without any mechanical disturbance. The closed container was recharged with H_2S gas in 6–8 h interval of time. Then the mineralization process is set for 4–6 days without any mechanical disturbance at room temperature. The sulphide minerals thus formed were collected by vacuum filtration washed with Milli-Q water several times to remove the organic additives, and then finally washed with cold anhydrous ethanol. The crystals are air-dried and kept in a desiccator for 24 h before analysis.

2.4 *Characterization techniques*

^{1}H NMR and ^{13}C NMR were recorded on a Varian FT-400 MHz instrument. Elemental analyses were done using Perkin–Elmer series II 2400 instruments. Scanning electron micrograph (SEM) images were obtained by means of a LEO-1430 VP electron microscope on samples glued on an aluminum stub and gold sputtered. FT–IR analysis was carried out on air-dried minerals samples. Because of the importance of knowing the polymorphs associated to crystalline structure, FT–IR measurements were performed. All spectra recorded at 4 cm^{-1} resolution with 10 scan with a Perkin Elmer-Spectrum One FT–IR Spectrometer from 4000 to 400 cm^{-1}. A background spectrum was measured for pure KBr. To confirm the crystalline nature of the mineral sample, PXRD data were recorded with Seifert powder X-ray diffractometer (XRD 3003TT) with CuK_α source (λ = 1·54 Å) on glass surface of air-dried sample. In order to determine presence of organic matrices and nature of polymorphs in the obtained mineral crystals, the samples were analysed thermally from 25 to 600°C using a DT-40 thermal analyser. The temperature was increased at a rate of

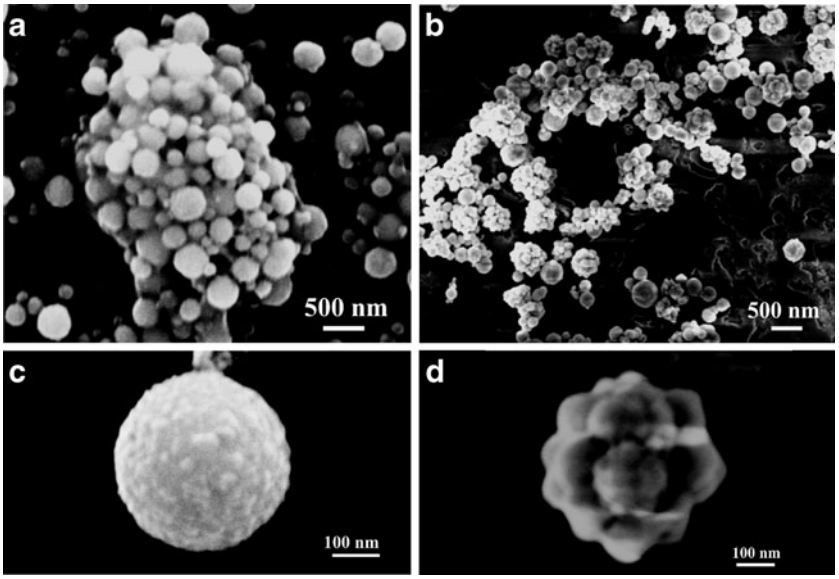

Figure 1. SEM images of CdS in presence of **a**. L_1, **b**. L_2, **c**. L_3 and **d**. L_4.

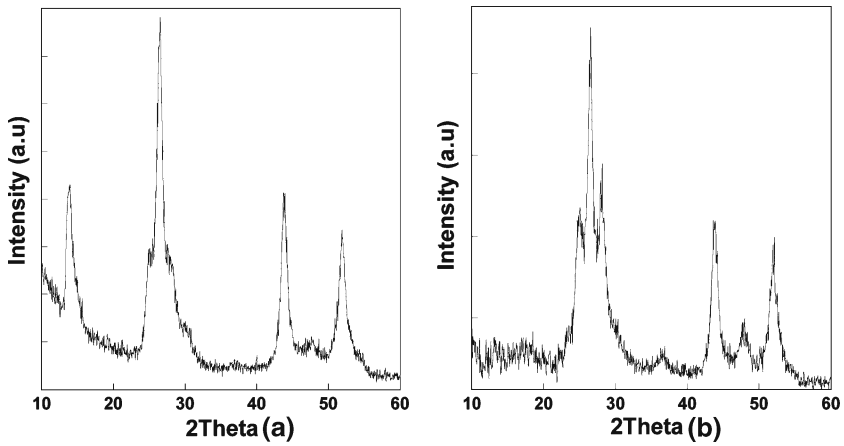

Figure 2. PXRD pattern of CdS from **(a)** L_3 and **(b)** L_4.

2 °C/min. UV-Vis absorption spectra of the samples are obtained on Perkin–Elmer lambda-25 spectrophotometer equipped with a dual-channel diffuse reflectance attachment. The PL measurements are carried out on a Varian Cary-Bio spectrometer.

3. Results and discussion

An *in vitro* study of biomineralization provides useful information for the design of organic templates. Model systems, in which low-molecular-weight organic additives are used to study the effect of crystal growth modification on inorganic mineralization, provide useful insights into the possible mechanisms operating in nature. Since the proteins that have been found to be associated with biomineralization are usually highly acidic macromolecules, simple water soluble chiral polycarboxylate ligands were examined as models of biomineralization in aqueous solution. These small organic molecules initially form a weak and flexible complex with the $Cd^{2+}/Pb^{2+}/Zn^{2+}$ ions or better we can say as a nucleation centre. This metal complex in turn acts as the nucleus for the crystal growth. The following sections describe our recent research on crystal nucleation and growth of few sulphide minerals in aqueous solution using low-molecular-weight polycarboxylate ligands.

3.1 *Crystallization of cadmium sulphide*

The cadmium sulphide formation in the solution can be observed as an increase in the yellow turbidity of the solution with time. Initially it forms a very thin yellow layer at the air–water interface and with time, CdS precipitated from the aqueous solution. The SEM pictures of CdS in the presence of organic matrix are shown in figure 1. In the presence

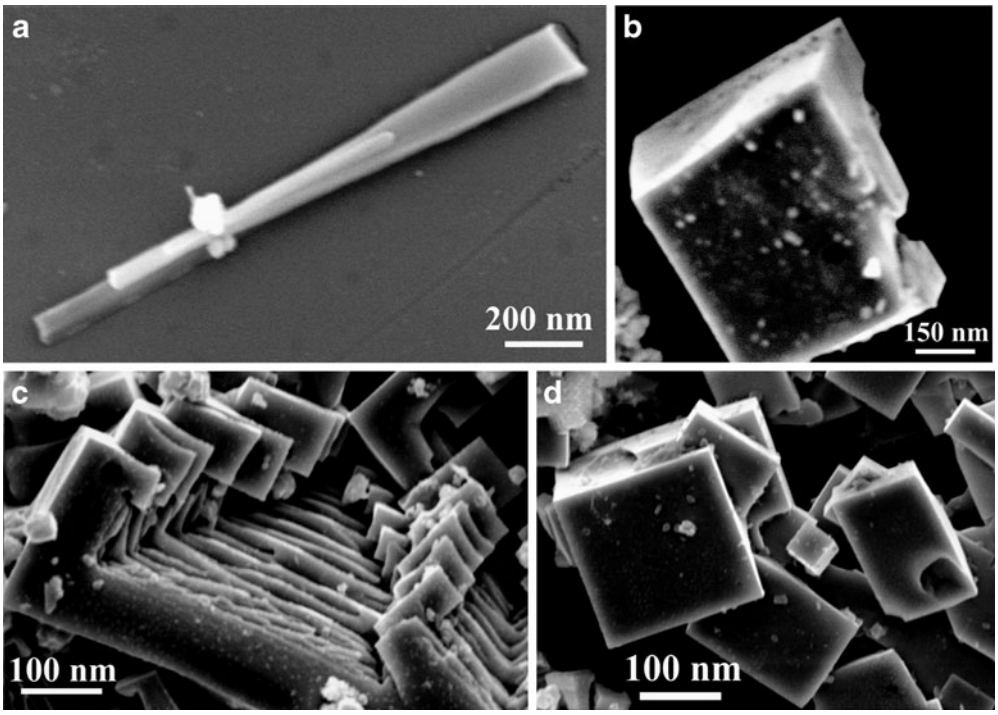

Figure 3. SEM images of PbS in presence of **a**. L_1, **b**. L_2, **c**. L_3 and **d**. L_4.

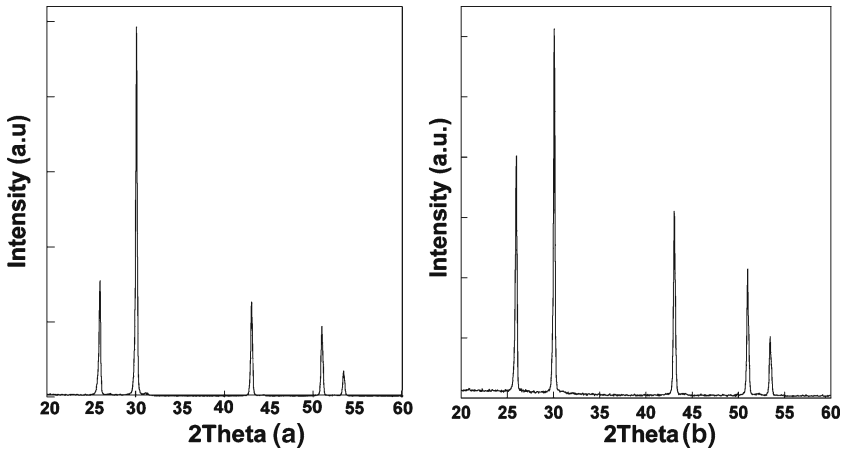

Figure 4. PXRD pattern of PbS from **(a)** L_{1-3} and **(b)** L_4.

of L_{1-3}, we got spherical CdS particles. In L_{1-2} matrix, the diameter of these balls range between 100 and 500 nm. These particles are agglomerated in the reaction condition. However, the size distribution of these spheres is narrow in case of L_3. It is in the range of 300–400 nm. In L_4 matrix, it forms a flower shape. The average width of the petals are < 100 nm. Elemental analysis (EDAX) shows the presence of CdS in all the cases. TGA analysis shows that no organic molecules are attached to the solid mineral. PXRD pattern of bulk CdS sample shows the presence of howleyite mineral phase in the presence of ligand L_1 (PDF No. 01-042-1411) and L_2 (PDF No. 01-075-1546). In the presence of L_3, it forms greenockite, Syn (PDF No. 00-041-1049) and in the presence of L_4 it forms greenockite, α-CdS (PDF No. 00-001-0783) mineral phase, respectively (figure 2).

3.2 *Crystallization of lead sulphide*

In our experimental condition, we have seen that initially a grey shiny thin layer of PbS is formed at the air–water interface. Within few hours, it changes to a black heavy

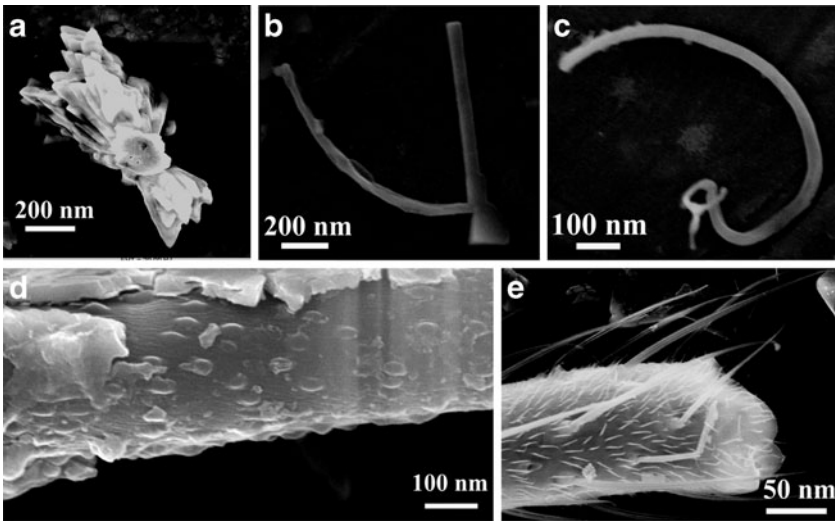

Figure 5. SEM images of ZnS in presence of **a**. L_1, **b**. L_2, **c**. L_3, **d**. L_4 (after 2 days) and **e**. L_4 (after 5 days).

precipitate of PbS. If we increase the concentration of organic matrix to 0·005 M, there is no appreciable change in the morphology of lead sulphide. However, if we increase the concentration of lead salt, then immediate precipitate of amorphous PbS is formed with any regular shape. The SEM picture of PbS in the presence of organic matrix are shown in figure 3. In L_1, it forms rods with an average length of 1 μm and width of the rods are in the range of 50–150 nm. From L_2 PbS rhombohedra has formed with a dimension range 150–500 nm. In the presence of L_3, PbS plates are formed. Width of these plates is in the range of 50–100 nm and average thickness is 15 nm. These plates are stacked on top of each other. From L_4 we got interpenetrated PbS rhombohedra. Dimension of these boxes are in the range of 100–250 nm. Elemental analysis (EDAX) shows the presence of PbS in all the cases. TGA analysis shows that no organic molecules are attached to the PbS mineral. In L_{1-3}, galena, syn is formed which matched with the PDF No. 03-065-0241. In the presence of L_4 it forms galena (PDF NO. 01-077-0244) mineral phase (figure 4).

3.3 *Crystallization of zinc sulphide*

Zinc sulphide formation in the aqueous solution phase can be observed by formation of faint dirty white turbidity followed by slow precipitation. The SEM picture of ZnS in the presence of L_{1-4} are shown in figure 5. From L_1, we got bundles of ZnS plates. Each plate has a common point of origin. Tip of each plates are also sharp. The width of these plates is in the range of 50–100 nm. In L_{2-3}, ZnS nano rods are formed. The average diameter of these rods is 50 nm. Close observation of the surfaces reveals that they are smooth and clean. However, in L_4 we got rods with a diameter range 100–400 nm. In contrast to the rods formed in case of L_{2-3}, here the surfaces are not smooth. Initially within two days, there are some random growths on the surface of these rods. Within 5 to 7 days, nano fibres grow from these regions. Average diameters of these fibres are <10 nm. Elemental analysis (EDAX) shows the presence of ZnS in all the cases. TGA analysis shows that no organic molecules are attached to the solid mineral. PXRD pattern of bulk ZnS sample shows the presence of zinc blende, syn (PDF No. 03-065-5476) in the presence of all (figure 6).

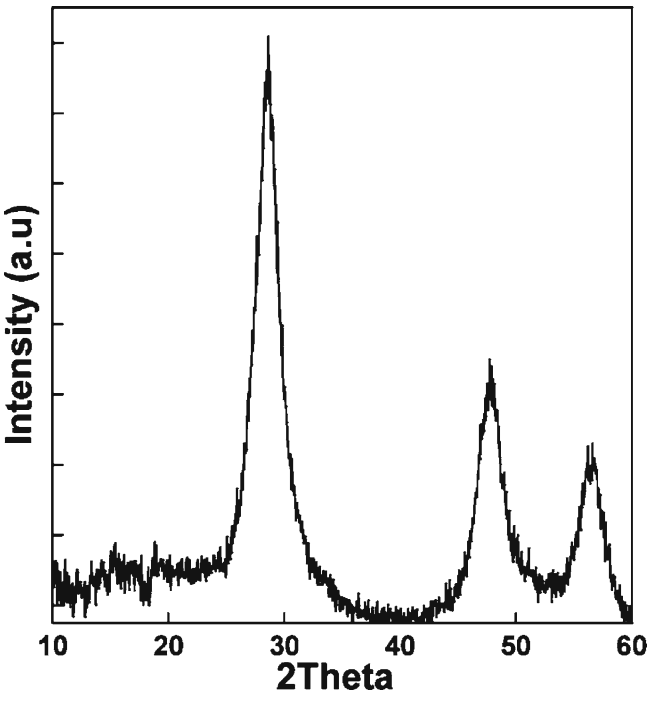

Figure 6. PXRD pattern of ZnS.

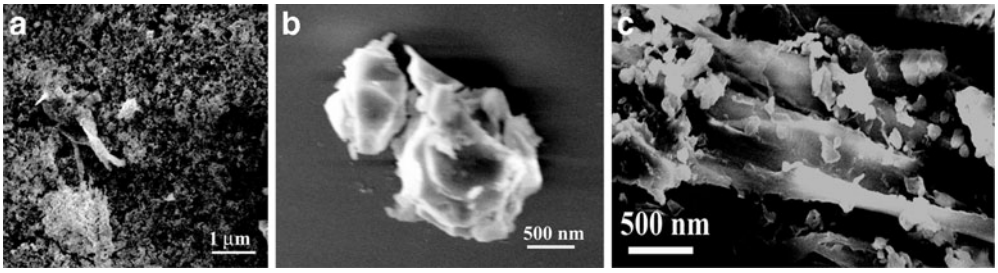

Figure 7. SEM of **a**. CdS, **b**. PbS and **c**. ZnS formed in the control experiments.

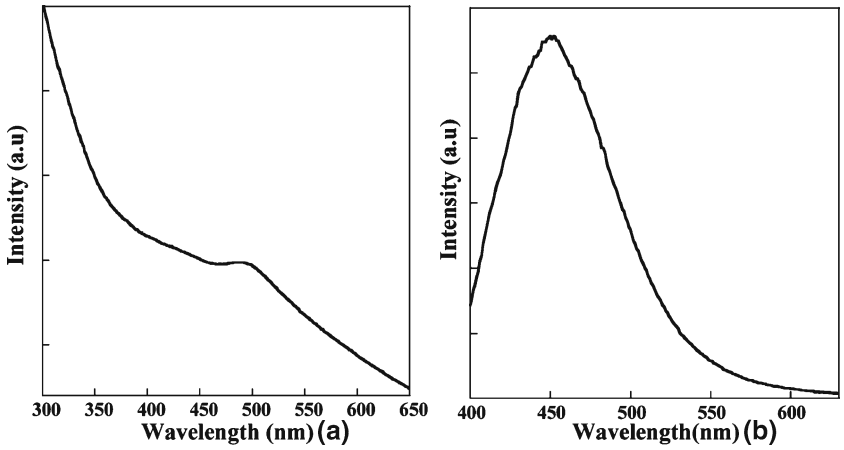

Figure 8. **(a)** UV-visible spectra and **(b)** PL spectra of CdS.

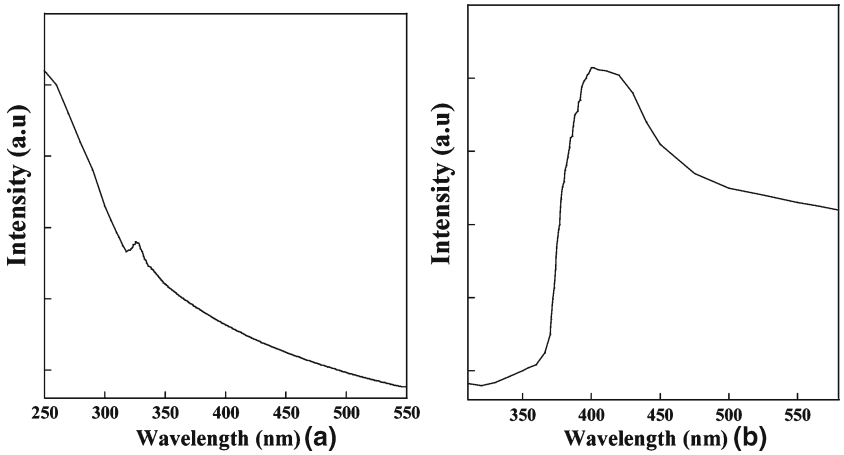

Figure 9. **(a)** UV-visible spectra and **(b)** PL spectra of ZnS.

3.4 *Control experiments*

In the control experiments, we have used simple amino acid as organic matrix. In all cases, we have found the formation of amorphous or agglomerated sulphides without any regular shape. Figure 7 shows some of the representative SEM pictures of the control experiments.

3.5 *Spectral characterization of sulphide minerals*

UV-Vis absorption spectroscopy is a useful technique to monitor the optical properties of the small particles. The room temperature UV-Vis absorption and PL spectra of CdS dispersed in dry THF are recorded and shown in figure 8. A maximum absorption peak at 495 nm in UV-Vis absorption

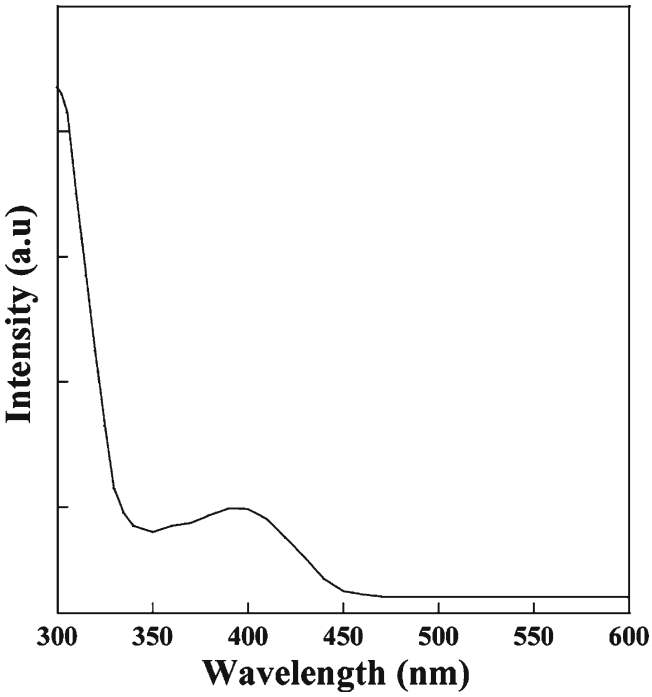

Figure 10. UV-visible spectra of PbS.

(figure 8(a)) is assigned to that of the first excitation state. The obvious blue shift compared to the reported data of bulk CdS (Gao *et al* 2002) results from the nanoparticles forming the microsphere. The absorption spectra of bulk CdS have an onset at 512 nm (2·4 eV). The PL spectrum of the CdS spheres is shown in figure 8(b), which exhibits a broad emission peak, centred around 450 nm, blue-shifted considerably from the emission of bulk CdS (520 nm). It is suggested that the emission peak at 450 nm is attributed to transition from conduction band to valence band. The emission peak blue shifts due to the quantum confined effect (Tang *et al* 2005).

Figure 9 shows the optical absorption and photoluminescence spectra of the ZnS rods. An absorption peak appears at ∼326 nm and has a modest blue shift (∼19 nm) compared to corresponding peak from bulk ZnS (345 nm) (Ma *et al* 2004), indicating that the bandgap energy (E_g) of ZnS rods was 3·8036 eV, which was much larger than that of the bulk ZnS (3·66 eV). This blue-shift could be attributed to smaller size of the ZnS rods. The PL spectrum shows a broad emission band centred at ∼400 nm (λ_{ex} = 300 nm), the peak corresponds to the bandgap emission of 3·1 eV, a blue-shift (∼40 nm) of the emission band position relative to the bulk ZnS (440–500 nm) is observed.

The UV-vis absorption spectrum of the as-prepared PbS is shown in figure 10. It can be seen that the UV-vis absorption edge is nearly 400 nm, and shows a very significant blue shift from the bulk PbS crystals (Ye *et al* 2005). The optical bandgap energies of PbS have been estimated to be 3·1 eV, showing obvious increment as compared with that of bulk PbS (0·37 eV).

4. Conclusions

In conclusion, polycarboxylate chiral ligands of low-molecular weight derived from naturally occurring *L*-α-amino acids form the matrix and influence the growth of the minerals. A preliminary study of these polyacidic ligands as matrices in the growth of sulphide minerals of cadmium, lead and zinc has been tested. Moreover, understanding the formation mechanism of the remarkable architecture should develop chemistry for manufacturing micron- and nanoscale functional materials in solution systems. From a technological point of view, this simple method is expected to allow fabrication of other inorganic materials with the controllable phases and shapes. Ligand L_4, derived from *L*-methionine, bearing sulfur atom in the side arm proved the best matrix for the crystal growth modifier among these four ligands. Because all these metal ions are expected to bind the soft sulfur donor atom more strongly. Nonpolar side chains containing amino acid derivatives are not good matrices for mineralization processes.

Supporting information

FT–IR spectra and EDX plots are available with us as supporting information.

Acknowledgements

This work was supported by CSIR and DST through grant 01-2235/08/EMR-II and SR/S1/IC-01/2008, New Delhi, India. (HT) is thankful to CSIR for JRF. We are thankful to the Central Instrumental Facility and Nanotechnology Centre of IIT Guwahati for extending their facilities.

References

Alivisatos A P 1996 *Science* **271** 933
Barnett R and Landman U 1997 *Nature* **387** 788
Borah B M, Bhuyan B J and Das G 2006 *J. Chem. Sci.* **118** 519
Chen S H and Carroll D L 2002 *Nano Lett.* **2** 1003
Gao F, Lu Q, Xie S and Zhao D 2002 *Adv. Mater.* **14** 1537
Grus M and Sikorska A 1999 *Physica B* **266** 139
Hu J, Odom T W and Lieber C M 1999 *Acc. Chem. Res.* **32** 435
Khanna P K, Gokhale R R, Subbarao V V V S, Singh N, Jun K W and Das B K 2005 *Mater. Chem. Phys.* **94** 454
Kuang D B, Xu A W, Fang Y P, Liu H Q, Frommen C and Fenske D 2003 *Adv. Mater.* **20** 1747
Labrenz M *et al* 2000 *Science* **1744** 290
Liu J W, Shao M W, Chen X Y, Yu W C, Liu X M and Qian Y T 2003a *J. Am. Chem. Soc.* **125** 8088
Liu Z P, Yang Y, Liang J B, Hu Z K, Li S, Peng S and Qian Y T 2003b *J. Phys. Chem.* **107** 12658
Ma Y R, Qi L M, Ma J M and Chang H M 2004 *Cryst. Growth Des.* **4** 351

Mann S, Archibald D D, Didymus J M, Douglas T, Heywood B R, Meldrum F C and Reeves N J 1993 *Science* **261** 1286

Mo M S, Zeng J H, Liu X M, Yu W C, Zhang S Y and Qian Y T 2002 *Adv. Mater.* **22** 1658

Panda S K, Datta A and Chaudhuri S 2007 *Chem. Phys. Lett.* **440** 235

Pentimalli M, Antolini F, Bauer E M, Capitani D, Luccio T D and Viel S 2005 *Mater. Lett.* **59** 3181

Puntes V F, Krishnan K M and Alivisatos A P 2001 *Science* **291** 2115

Raji P, Sanjeeviraja C and Ramachandran K 2005 *Bull. Mater. Sci.* **28** 233

Sun Y G and Xia Y N 2002 *Science* **298** 2176

Suresh Babu K, Ranjith Kumar T, Haridoss P and Vijayan C 2005 *Talanta* **66** 160

Tang H, Yan M, Zhang H, Xia M and Yang D 2005 *Mater. Lett.* **59** 1024

Wang D B, Mo M S, Yu D B, Xu L Q, Li F Q and Qian Y T 2003 *Cryst. Growth Des.* **3** 717

Wang X and Li Y D 2003 *Chem. Eur. J.* **9** 300

Winter J O, Gomez N, Gatzert S, Schmidt C E and Korgel B A 2004 *Colloid Surface A* **254** 147

Xia Y N and Yang P D 2003 *Adv. Mater.* **15** 351

Xie Y, Qiao Z P, Chen M, Liu X M and Qian Y T 1999 *Adv. Mater.* **11** 1512

Xiong Y J, Xie Y, Li Z Q, Li X X and Gao S M 2004 *Chem. Eur. J.* **10** 654

Yang P D and Lieber C M 1996 *Science* **273** 1836

Ye S, Ye Y, Ni Y and Wu Z 2005 *J. Cryst. Growth* **284** 172

Yu J C, Xu A W, Zhang L Z, Song K Q and Wu L 2004 *J. Phys. Chem. B* **108** 64

Zhang J, Sun L D, Jiang X C, Liao C S and Yan C H 2004 *Cryst. Growth Des.* **4** 309